Electron Spin Resonance Studies on Sodium-Neutralized Ethylene Ionomers: Microphase-Separated Structure and Thermal Behaviors

Shoichi Kutsumizu,* Masahiro Goto, and Shinichi Yano

Department of Chemistry, Faculty of Engineering, Gifu University, 1-1 Yanagido, Gifu 501-1193, Japan

Received December 23, 2003

ABSTRACT: Electron spin resonance (ESR) spectroscopic measurements using nitroxide spin probes were performed to investigate the microphase-separated structure of sodium-neutralized poly(ethylene-*ran*-methacrylic acid) [E−MAA] ionomers as a function of temperature from 77 to 403 K. It was found that the probes selected are intercalated position-selectively into the ionomers, and information about the local chain mobility around those probes was successfully obtained from the extreme separation of the spectra. Their temperature variation indicated which site is changed when temperature is varied through three characteristic temperatures of the ionomers (glass transition of the backbones [$T_g \approx 230-240$ K], ionic aggregate transition [$T_i \approx 320$ K], and polyethylene lamellae melting [$T_m \approx 360$ K]). The results demonstrated that the effect of an ionic aggregate on the chain mobility becomes larger and extends to a longer distance from the aggregate at the higher degrees of neutralization x; at $x = 0.8$ and 0.9, the spectra of spin probes located in the amorphous region showed the presence of two dynamical states, corresponding to the matrix and ionic cluster phases in the Eisenberg et al. terminology, and the restricted mobility of the chains in the cluster phase persisted beyond T_m. On the other hand, the spectra of the probes deeply intercalated into the aggregate core clearly changed at T_i for $x \geq 0.6$, accompanied by a characteristic thermal hysteresis similar to the behavior of the DSC T_i peak. This result clearly supports the model of an ionic aggregate transition proposed by us previously.

Introduction

Poly(ethylene-*ran*-methacrylic acid) [E−MAA, shown in Chart 1a] ionomers neutralized with metal cations are industrially important materials with many applications for packaging, coatings, adhesives, and others.[1−3] The materials performances are closely related to the structure, and the morphology of the E−MAA ionomers is interpreted as a three-phase model consisting of crystalline lamellae, amorphous region, and ion-rich domains called ionic aggregates.[4−6] The presence of the third region, ionic aggregates, is crucial for improving the polymer properties compared to the host polymer polyethylene. However, the three regions are interconnected with each other,[7] and especially, the presence of crystalline lamellae makes E−MAA ionomers very complicated materials. Despite a large number of studies documented on E−MAA ionomers for more than 3 decades, several fundamental issues have remained unsolved regarding the structure and nature of the ionic aggregates.

An important but unsolved issue is the origin of an anomaly observed at ≈320 K (denoted as T_i in this paper) below the melting temperature of polyethylene lamellae ($T_m \approx 360$ K).[8−21] On heating immediately after cooling from the melt, the differential scanning calorimetric (DSC) scan exhibits only an endothermic peak at T_m, but when aged at room temperature for more than several days, an additional endothermic peak is observed at ≈320 K on heating; the size of the T_i peak increases with the aging time. There have been proposed three assignments for the peak, i.e., the melting of imperfect polyethylene crystallites (secondary crystallites),[8−10,19,20] the release of absorbed water from the ionic aggregates,[17] and an order−disorder transition of ionic aggregates,[11−16,18,21] but no definitive evidence has

Chart 1

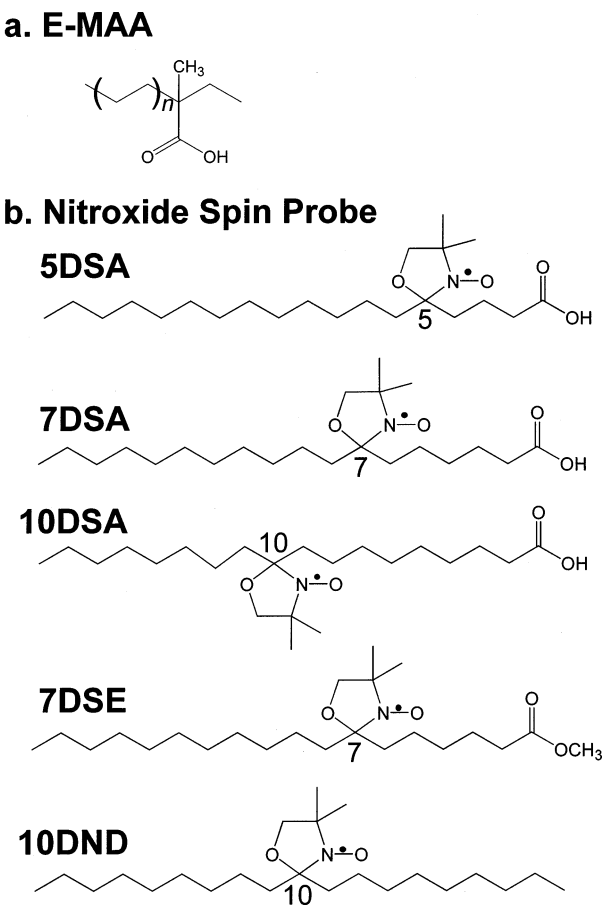

* To whom correspondence should be addressed. E-mail: kutsu@cc.gifu-u.ac.jp.

10.1021/ma0305885 CCC: $27.50
Published on Web 06/03/2004

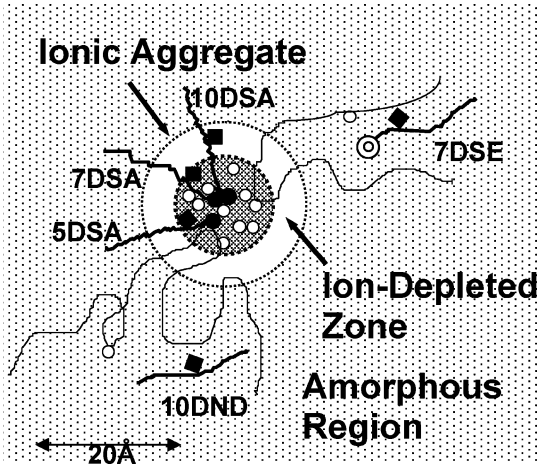

Figure 1. Suggested locations of 5DSA, 7DSA, 10DSA, 7DSE, and 10DND probes in dry E−MAA ionomers, based on the analysis of ESR studies;[33] the carboxylate and carboxylic acid groups of the ionomers (○), the acid groups (●), the methyl ester group (◎), and the nitroxide groups (■) of the probes are indicated. Dark shaded, white, and gray-shaded regions represent respectively the ionic core and hydrocarbon shell (ion-depleted zone) of the aggregate and the amorphous region.

selected one of these models. This is partly due to the nanometer size of the ionic aggregate region and partly due to the interconnection of the three regions in the ionomer.[7] Related to the anomaly, earlier birefringence,[22] X-ray diffraction,[23] and infrared dichroism[24] studies by MacKnight and co-workers proposed the presence of a softening temperature of ion-rich domains at a temperature very close to T_i, but they did not refer to the relation to the DSC T_i peak in the papers. The picture of the softening temperature of ion-rich domains is, however, very similar to the third assignment, an order−disorder transition model of the ionic aggregates. On the other hand, Hirasawa et al. pointed out that the size of the DSC T_i peak seems to be correlated with some performances of the ionomers such as yield strength, surface hardness, and bending modulus;[13,14,18] the bending modulus, for example, of a zinc(II)−amine complex salt of E−MAA ionomer containing 5.4 mol % MAA is 200 MPa immediately after cooling from the melt but increases up to 450 MPa, about 2.3 times, after being agied at room temperature for 38 days.[13] Therefore, understanding the origin of the DSC T_i peak is important not only from an academic point of view but also from an industrial viewpoint.

Electron spin resonance (ESR) spectroscopy is an important tool for probing the local environment around species containing unpaired electrons. Early ESR studies in ionomers analyzed the spectra from paramagnetic transition-metal cations and obtained the local coordination structure, but recent advanced studies have obtained the local molecular dynamics in ionomers by using spin probe techniques and double electron−electron resonance spectroscopy.[25−33] Our group has recently studied the morphology and local structure in dry E−MAA ionomers.[33] In the studies, the following five spin probes as shown in Chart 1b were selected: four probes (5DSA, 7DSA, 10DSA, and 7DSE) are based on stearic acid, and one (10DND) has a nonadecane chain; the number at the top of each probe notation represents the nitroxide group position, i.e., the ESR probe site. An important conclusion obtained is position selectivity of those five probes in the ionomers, as schematically illustrated in Figure 1: Three hydrophilic *n*DSA probes, with $n = 5$, 7, and 10, have a COOH group at the terminal which is directly anchored to the ionic aggregate through ionic interactions; the distances from the center of the aggregate to their nitroxide groups were estimated to be 6.6, 9.8, and 12.4 Å for 5DSA, 7DSA, and 10DSA, respectively. Two hydrophobic 7DSE and 10DND would be excluded from both ionic aggregate and polyethylene lamellae regions, located at the hydrophobic amorphous region. Furthermore, the analysis of the polarity index (ΔA_0) has revealed that the nitroxide group of 10DSA is located in the region where almost all ionic groups are excluded to leave only polyethylene segments; this region was considered to correspond to the hydrocarbon shell of the ionic aggregate (ion-depleted zone). The locations of *n*DSA as "dipsticks" in the aggregate were consistent with the size characteristics deduced from the small-angle X-ray scattering (SAXS) measurements within a few angstroms.[33]

By using these position-selective spin probes, this paper aims at obtaining information about the local molecular dynamics in the E−MAA ionomers as a function of temperature. For this purpose, the extreme separation of outer peaks of the ESR spectrum ($2A'_{zz}$) is used as a measure for the chain mobility around the probes. Such information is important on its own and also expected complementary with the dielectric and dynamic mechanical results on the same system.[34] Moreover, it is expected to obtain a more clear insight into the DSC T_i peak at ≈320 K, which is subject to debate, and also which region is responsible for the gradual change of the physical properties during the room temperature aging, mentioned above.

Experimental Section

Materials. The spin probes were purchased from Aldrich and used as received. E−MAA ionomers were a gift from Technical Center, Du Pont-Mitsui Polychemicals Co., Ltd., Chiba, Japan. The ionomer precursor E−MAA, with M_n = 19 000 and M_w = 95 000, contained 5.4 mol % MAA units in the backbone, and the melt index (MI) was 60 g/10 min. The average number of backbone carbons between two neighboring COOH groups was therefore ≈36 (the *n* of Chart 1a is ≈17.5). The COOH groups were partially neutralized with Na, and the obtained ionomers are denoted as E−MAA-*x*Na, where *x* is the degree of neutralization ($0 \le x \le 1$). The detailed neutralization procedure has been reported.[14] Low-density polyethylene (LDPE), with the density of 0.923 g cm^{-3}, MI = 3.7 g/10 min, M_n = 31 000, and M_w = 326 000, was from Mitsui Chemicals Co., Ltd., Chiba, Japan.

The spin probes were intercalated into the samples by dipping the sample films into the aqueous probe solutions/dispersions of ≈0.1 mM at room temperature, using the procedure described previously.[25,27,28] The sample films were then dried in a vacuum oven at 403 K for 2 h[15] and sealed into quartz tubes under vacuum. Thus, all the samples containing spin probes were water-free. Water absorption during the storage at ambient temperature would make the analysis of the structural evolution with storage time complicated,[15,17,18,21] but such doubt was eliminated in our studies. The concentration of the spin probes in the samples was adjusted and low enough to avoid line width broadening due to spin−spin interactions; the probe concentration was roughly estimated, and the ratio [COO$^-$/COOH]/[spin probe] was 10^3−10^4. The very low concentration can also minimize the influence of the probe molecules on the polymer chain dynamics as much as possible.

Measurements. ESR spectra at various temperatures were measured with a JEOL JES-TE200 X-band spectrometer equipped with an ES-DVT3 variable-temperature unit. In the temperature range below 273 K, temperature (*T*) was elevated

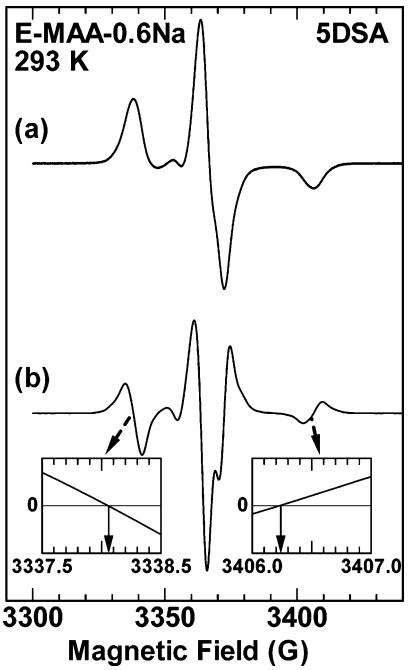

Figure 2. (a) First-derivative and (b) second-derivative ESR spectra of 5DSA in E−MAA-0.6Na at 293 K. In (b), two insets enlarge the vicinity of the pattern where the second derivative crosses zero.

every 10 K, and the samples were allowed to equilibrate for about 5 min prior to the measurement after T reached a preset temperature. The overall heating rate was 0.25−0.5 K min^{-1}. In the temperature range 273−403 K, the heating rate was slightly higher and about 1 K min^{-1}; this rate might not be slow enough for slow reorganizations characteristic of polymers but would make an easy comparison with the corresponding DSC scan recorded at 10 K min^{-1}. In separate experiments, ESR spectra were monitored with time at a constant T to confirm the presence of the annealing effect. The spectra at 77 K were measured in a liquid nitrogen finger dewar inserted in the cavity. At all temperatures, care was taken to avoid the deformation of the spectral pattern by the power saturation effect; the power P was adjusted to allow a linear relation of the ESR intensity with $\sqrt{P}$. The P used were 0.02 mW (T = 77 K), 0.05 mW (153 K ≤ T < 203 K), 0.1 mW (203 K ≤ T < 223 K), 0.2 mW (223 K ≤ T < 263 K), 0.5 mW (263 K ≤ T < 283 K), and 1.0 mW (283 K ≤ T).

The following thermal cycles were used to examine the temperature variations of the ESR spectra: The starting sample for the first heating (1h) scan was aged at 293 K for about 30 days after cooling from the melt at a rate of ≈10 K min^{-1}. After the 1h scan up to 403 K, the sample was cooled to 273 K at a rate of ≈10 K min^{-1} without measurements, and then, the second heating (2h) scan was performed up to 403 K, followed by the second cooling (2c) scan down to 273 K. Note that the 2c scan corresponds to the first cooling scan from the melt measured by DSC. After that, the sample was again heated to 403 K in the melt, cooled to 273 K at a rate of ≈10 K min^{-1}, and aged at 293 K for 30 days for the next measurement at 293 K; the final state of the sample prepared in this way would be identical with the initial state at 293 K in the 1h scan.

Digital encoding of the spectral data was transferred into a personal computer and handled by using Microsoft Excel and Visual BASIC. Figure 2 shows an example of such data treatments. Patterns a and b are first- and second-derivative spectra at 293 K for 5DSA intercalated into E−MAA-0.6Na. The second derivative was obtained after smoothing the first-derivative spectrum (raw data), and thus it was possible to determine the value of the extreme separation of outer peaks ($2A'_{zz}$) in the first-derivative pattern, i.e., the distance between two points at which the second derivative is zero, within an uncertainty of ±0.3 G (if the pattern consists of one component).

DSC thermograms were recorded by using a Seiko Denshi DSC-210 calorimeter (SSC-5000 system), which was calibrated by standard materials (In, Sn, Pb, and Zn). The measurements were done at a rate of 10 K min^{-1} under a dry N_2 flow of ca. 40 mL min^{-1}. As mentioned in the Introduction, partly crystalline E−MAA ionomers aged at room temperature for about 30 days exhibit two endothermic peaks at ≈320 K (assigned to the T_i) and ≈360 K (T_m) on the first heating. The weight fraction of polyethylene crystallinity (X_c) was calculated from the enthalpy change at T_m by assuming that the heat of fusion of polyethylene crystallites is 290.4 J g^{-1}. On cooling from the melt, only one peak appears originating from the crystallization of polyethylene segments, the temperature of which is denoted as T_c, and the subsequent heating exhibits the T_m peak only. Table 1 summarizes the DSC parameters for the samples examined in this paper.

SAXS measurements were carried out at the Photon Factory (PF) beamline BL-10C, the National Laboratory for High Energy Physics (KEK), Tsukuba, Japan. The synchrotron radiation with λ = 1.488 Å and point-focusing optics were used. Details of the optics, measurements, and data treatments are described elsewhere.[35] Two camera distances, 201.6 and 62.0 cm, were used to cover q in the range 0.02−0.17 and 0.1−0.7 Å^{-1}, respectively. Here, $q = (4\pi/\lambda) \sin\theta$, and λ (=1.488 Å) and 2θ are the wavelength and scattering angle, respectively, of the X-rays.

Results

Temperature Variation of $2A'_{zz}$ for E−MAA-0.6Na. Figure 3 shows selected ESR spectra of five probes in E−MAA-0.6Na in the temperature range 77−393 K on heating, and on the right side of each spectrum, the value of the extreme separation of outer peaks ($2A'_{zz}$) is shown. At 77 K, the spectra for all probes have a very broad line shape, consisting of one component. The spectral shape clearly indicates that the molecular motion of those probes is virtually frozen out; the values of $2A'_{zz}$ at 77 K (which were distinguished as $2A_{zz}$ in our preceding paper[33] in the sense of the rigid limit) are 69.4, 67.6, 66.7, 67.1, and 67.2 G for 5DSA, 7DSA, 10DSA, 7DSE, and 10DND, respectively. The uncertainty of the absolute values was ±0.3 G at maximum, but the relative errors of the same sample could be much reduced; thus, the trend of $2A'_{zz}$(5DSA) > $2A'_{zz}$(7DSA) > $2A'_{zz}$(10DSA) < $2A'_{zz}$(7DSE) ≈ $2A'_{zz}$(10DND) can be recognized. The same trend was also observed for x = 0.4, 0.8, and 0.9. As fully discussed in our preceding paper,[33] the trend observed directly reflects the change in polarity from the inside of the aggregate core to the hydrocarbon shell and to the surrounding amorphous region; the probe site of 10DSA is located at the hydrocarbon shell, where most of ionic groups are excluded (see Figure 1). The location of the probes deduced will be further supported by the temperature variations of the $2A'_{zz}$ values of those probes to be mentioned below.

In the temperature range 77−293 K, the variation of the spectral pattern with increasing temperature is very gradual for all probes. As temperature is raised beyond 293 K, the spectra of 7DSA, 10DSA, 7DSE, and 10DND begin to evolve toward a motionally averaged triplet pattern with the $2A'_{zz}$ of ≈32 G. The most prominent change is seen at ≈360 K, corresponding to the melting of polyethylene lamellae region (the temperature T_m = 361.6 K measured by DSC for E−MAA-0.6Na); this region acts as a physical cross-link of the ionomer chains and restricts the local molecular motion around those four probes below T_m. A close look at the patterns of

Table 1. DSC Parameters for Various Sodium-Neutralized E−MAA Ionomers[a]

ionomers	T_i/K	ΔH_i/J g^{-1}	T_m/K	ΔH_m/J g^{-1}	X_c/%	T_c/K	ΔH_c/J g^{-1}
LDPE	−	−	384.6	130.7	45	371.5	120.1
E-MAA	314.6	5.5	363.8	81.4	28	333.0	69.1
E-MAA-0.2Na	315.1	7.4	364.4	76.2	26	336.3	69.0
E-MAA-0.6Na	321.3	16.6	361.6	42.2	15	322.3	34.7
E-MAA-0.9Na	321.3	13.8	361.0	15.0	5	314.5	13.4

[a] T_i, order−disorder transition temperature of ionic aggregates; ΔH_i, enthalpy change of the T_i peak; T_m, melting temperature of polyethylene crystallites; ΔH_m, enthalpy change of the T_m peak; X_c, percent crystallinity of polyethylene segments; T_c, crystallization temperature of polyethylene segments; ΔH_c, enthalpy change of the T_c peak; −, not found.

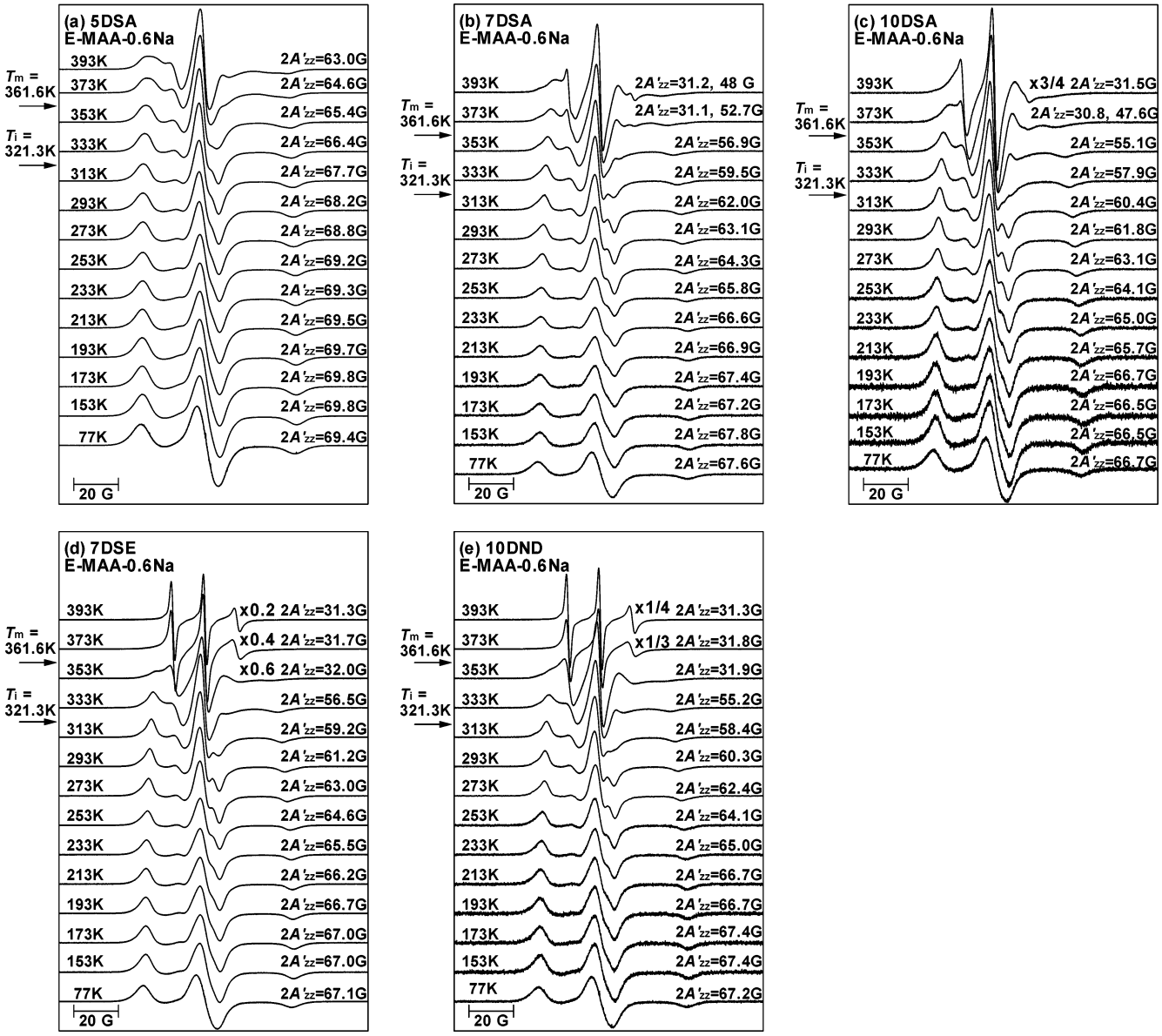

Figure 3. X-band ESR spectra of five probes in E−MAA-0.6Na as a function of temperature in the range 77−393 K: (a) 5DSA, (b) 7DSA, (c) 10DSA, (d) 7DSE, and (e) 10DND, where the spectra, normalized to a common frequency of 9.43 GHz, are shifted vertically, but the intensity relation is preserved except between 153 and 77 K. The modulation amplitude was 0.1 mT.

7DSA at 373 and 393 K and of 10DSA at 373 K show a superposition of two components: a motionally averaged and a motionally restricted component. Compared to those probes, the evolution of 5DSA is significantly different, with the $2A'_{zz}$ of 63.0 G even at 393 K above T_m, indicating that the local molecular motion around 5DSA is still strongly restricted at the temperature. Furthermore, very faint shoulder peaks in the outside of the outer peaks are seen for 7DSE and 10DND around room temperature (see also ref 33, Figure 3) but too faint to determine the position precisely. This splitting is much more clearly observed for E−MAA-0.9Na (Figure 8).

Figure 4 plots the $2A'_{zz}$ values of the five probes as a function of temperature (T). The $2A'_{zz}$ values of hydrophobic 7DSE and 10DND in the amorphous region are almost independent of temperature between 77 and ≈230 K, and when the temperature is raised above this temperature region, the values begin to decrease, which is clearly due to the glass transition (T_g) of the ionomer

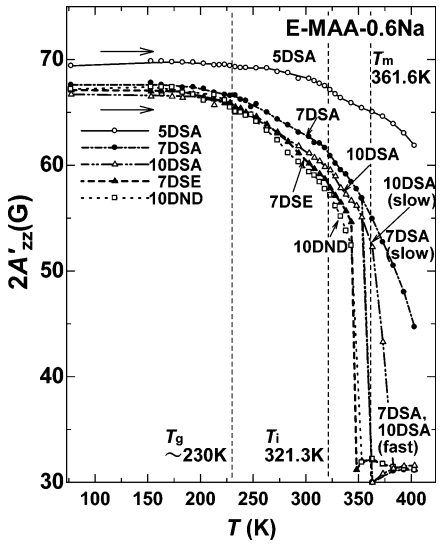

Figure 4. Plots of $2A'_{zz}$ vs temperature (T) in the range 77−403 K on heating for five probes in E−MAA-0.6Na. The curves in the figure are drawn to guide to the eye. The spectra of 7DSA and 10DSA consist of two components in a temperature range around 375 K, where two $2A'_{zz}$ values are plotted as slow and fast components (see text). T_g is the temperature at which the plots of $2A'_{zz}$ vs T for both 7DSE and 10DND show a bend, and T_i and T_m were determined by DSC.

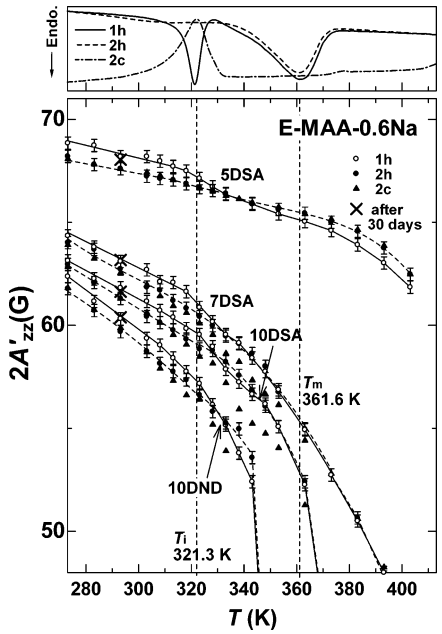

Figure 5. Plots of $2A'_{zz}$ vs T in the range 273−403 K on first heating scan (1h, ○), on second heating scan (2h, ●), and on second cooling scan from the melt at 403 K after the 2h scan (2c, ▲) for four probes in E−MAA-0.6Na; the fast counterparts of 7DSA and 10DSA around T_m are neglected for clarity. After these measurements, the samples were cooled from the melt to room temperature and aged for about 30 days, and then, the data × were recorded at 293 K. In the upper part of this figure, the corresponding DSC curves are shown.

backbones. The rate of the decrease slightly increases with increasing temperature. At ≈340 K, slightly lower than the T_m, those values suddenly drop to ≈32 G, indicative of a rather free and isotropic motion of the probes. The most hydrophilic 5DSA, on the other hand, shows a somewhat broad but definite steplike decrease at ≈320 K (which is more clearly seen in the next Figure 5), very close to the T_i (= 321.3 K, as measured by DSC), but with no drop at T_m, unlike other four probes. The $2A'_{zz}$ values of 7DSA and 10DSA also change at around T_i, and around T_m a coexistence of fast and slow components was observed.

The $2A'_{zz}$ vs T plots for the five probes in the temperature region 273−403 K are enlarged in Figure 5, where the plots of the fast components of 7DSA and 10DSA around T_m are omitted for clarity. This figure includes data on the first heating scan (1h), on the second heating scan (2h), and on cooling from the melt at 403 K after the 2h scan (2c). The corresponding DSC curves are shown in the same temperature scale in the upper part of Figure 5. It is evident that only the 1h scan for 5DSA shows a steplike change between 318 and 333 K, near T_i; the plots of both 2h and 2c scans, superposed with each other, are almost in a straight line up to ≈360 K and above this temperature slightly curved downward. A similar steplike anomaly is seen for 7DSA and 10DSA on the 1h scan, but less evident than the case for 5DSA; the difference of the $2A'_{zz}$ value at 293 K between 1h and 2h scans is ≈0.8 G for 5DSA, ≈0.6 G for 7DSA, and ≈0.3 G for 10DSA.

The second important point in Figure 5 is that the $2A'_{zz}$ values of five probes at 293 K on the 2h scan (●) is smaller than the corresponding values on the 1h scan (O), but after aging at 293 K for 30 days those values (×) were almost restored to the original 1h values. The increase in the $2A'_{zz}$ value with aging time reflects a reorganization occurring at each probe site at 293 K, which promotes immobilization of the chain segments therein. The reorganization occurs everywhere in the sample after cooling from the melt, but most evidently at the site of 5DSA, inside the core of the ionic aggregate.

The steplike change at T_i observed for 5DSA only on the 1h scan, not on both 2h and 2c scans, and a relaxation process at 293 K toward the initial state after cooling from the melt, which are more prominent compared to other four probes, are all consistent with the T_i anomaly with a thermal hysteresis observed by DSC (upper graph). This supports an order−disorder transition model of the ionic aggregate region proposed previously by our research group.[11−16,18,21]

Figure 6 shows SAXS patterns for E−MAA-0.6Na as a function of aging time at room temperature after being quenched from the melt, where the patterns were normalized with respect to the film thickness shown in parentheses. In this q region are seen the polyethylene lamellae peak around $q = 0.1$ Å^{-1} (in the upper graph) and the well-known ionic peak around $q = 0.3$ Å^{-1} (in the lower graph). In the lower graph, triplicate patterns measured immediately after quenching from the melt showed a maximum of 7% difference in the top intensity of the ionic peak, and the ionic peak profiles corresponding three different aging times coincide with each other within the experimental errors. This is indicative of no change in the size and shape and the space distribution of the ionic aggregates with aging time at room temperature. Therefore, it may be said that the aging at room temperature only gives rise to changes in the local molecular dynamics, especially in the vicinity of the ionic aggregates.

Temperature Variation of $2A'_{zz}$ for E−MAA-0.2Na. Figure 7 shows the $2A'_{zz}$ vs T plots for three probes in E−MAA-0.2Na on heating. In the upper graph, the DSC scans show an endothermic peak at 315.1 K only on the 1h scan, which was assigned to T_i, similarly to the case in E−MAA-0.6Na, but the size of

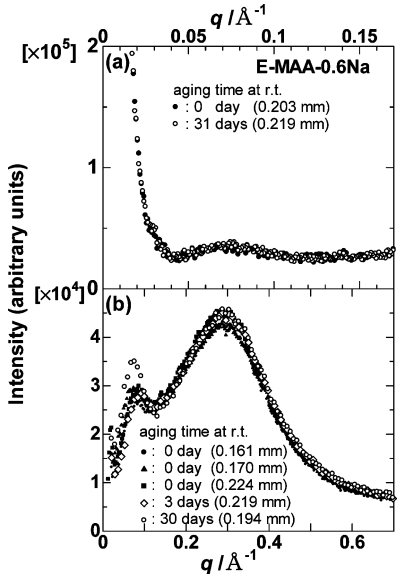

Figure 6. SAXS patterns of E−MAA-0.6Na aged at room temperature for different storage times; in the q range of (a) 0.015−0.17 Å^{-1} and (b) 0.02−0.7 Å^{-1}. In (b), scattering of the data points is seen below $q = 0.1$ Å^{-1} due to the resolution limit of the camera length used.

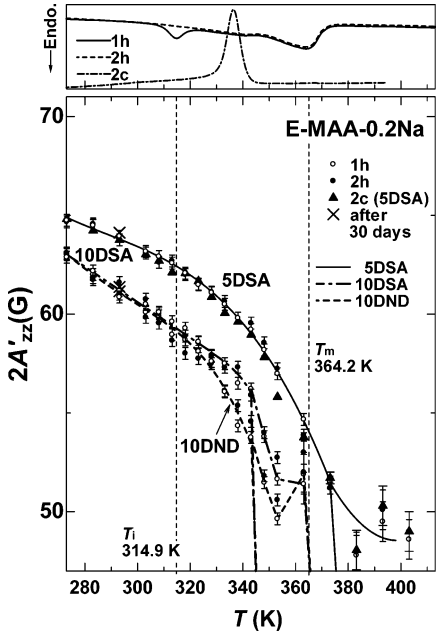

Figure 7. Plots of $2A'_{zz}$ vs T in the range 273−403 K on first heating (1h, ○), second heating (2h, ●), and second cooling (2c, ▲) for three probes in E−MAA-0.2Na; the 2c data of 10DSA and 10DND are omitted for clarity. ×, T_i, and T_m are the same as in Figure 5. The corresponding DSC curves are shown in the upper part of this figure.

the peak is much smaller than that in E−MAA-0.6Na. In the lower graph, as temperature is raised, the $2A'_{zz}$ value of 5DSA begins to drop at around the T_i and the major part finally reaches ≈32 G around 370 K, with a small portion of a motionally restricted component with the $2A'_{zz}$ of ≈48 G. Contrary to the case of E−MAA-0.6Na, no difference is seen among the three scans, 1h, 2h, and 2c. Apart from the plots for 5DSA, the $2A'_{zz}$ vs T plots for 7DSA, 10DSA, 7DSE, and 10DND were almost superposed with each other, and the three scans for the same probe could not be distinguished also. In Figure 7 are shown only the data for 10DSA and 10DND on the 1h and 2h scans for clarity. Those plots suddenly drop owing to the melting of polyethylene lamellae on heating, with a coexistence of two components between 348 and 363 K. Similar to 5DSA, no anomaly is visible at around T_i for those probes.

Our preceding paper[33] revealed that the polarity indices ΔA_0 of five probes, 5DSA, 7DSA, 10DSA, 7DSE, and 10DND, in the E−MAA-0.2Na range between 0.70 and 0.83. The narrow range of the ΔA_0 values and the results in Figure 7 all indicate that the microphase separation between the ionic and nonionic moieties in E−MAA-0.2Na ionomer does not proceed so much. This is of course reasonable considering that the neutralization level of this ionomer is much lower compared to that of E−MAA-0.6Na.

Temperature Variation of $2A'_{zz}$ for E−MAA-0.9Na. Figure 8 shows ESR spectra in the temperature range 77−393/403 K for (a) 5DSA and (b) 10DND in E−MAA-0.9Na.

The temperature variation of 5DSA in (a) is similar to that of the same probe in E−MAA-0.6Na (Figure 3a). The more interesting point is seen for 10DND in (b): as illustrated by two pairs of sticks, splitting of outer peaks is visible above 253 K. This splitting seems not prominent above 373 K in the intensity scale of (b) but does exist as shown in the upper spectrum of (c). A similar observation is seen also for 7DSE in the lower spectrum (the temperature variation not included).

The $2A'_{zz}$ vs T plots for hydrophilic 5DSA and hydrophobic 7DSE and 10DND in E−MAA-0.9Na on heating are shown in Figure 9, together with the plot for 10DND dispersed in LDPE for comparison. As temperature is raised, the $2A'_{zz}$ value of 5DSA initially decreases very gradually in the temperature range below ≈320 K, and at T_i (= 321.3 K, measured by DSC for E−MAA-0.9Na), a steplike decrease is visible, as seen in E−MAA-0.6Na (Figure 5). After that, the magnitude of the decrease with temperature slightly increases, but the value at 403 K is 65.7 G, still very large. Note that this value is larger than the value of E−MAA-0.6Na ($2A'_{zz}$ = 61.9 at 403 K) or of E−MAA-0.2Na ($2A'_{zz}$ ≈ 48 G for the motionally restricted component).

The $2A'_{zz}$ values of 7DSE and 10DND, on the other hand, are almost constant with temperature below 240 K; at 240 K, the splitting of the outer two peaks becomes evident. This temperature corresponds to the glass transition temperature of polyethylene backbones (T_g).[36] The spectra of the two probes at 77 K, at which the molecular motions of those probes are frozen out, consist of one component. Thus, not the difference in polarity but the difference in mobility around their microenvironments causes the splitting, and the larger and smaller $2A'_{zz}$ correspond to immobile and slightly mobile components, respectively. For both 7DSE and 10DND, the $2A'_{zz}$ values of the mobile components decrease almost linearly with temperature and at 350 K suddenly drop to ≈32 G. This reflects the melting of polyethylene lamellae (T_m = 361.0 K, measured by DSC for E−MAA-0.9Na). Actually, these behaviors are similar to that of 10DND in LDPE, except that in LDPE the temperature at which the $2A'_{zz}$ value drops is ≈320 K, by ca. 30 K lower.

The temperature variation of the immobile components is quite different from those of the mobile components. Since the spectrum of the immobile components is seen as a shoulder in the outer peaks, the error bar of ±1.0 G at maximum is shown in Figure 9 (but the relative errors of the same sample could be reduced).

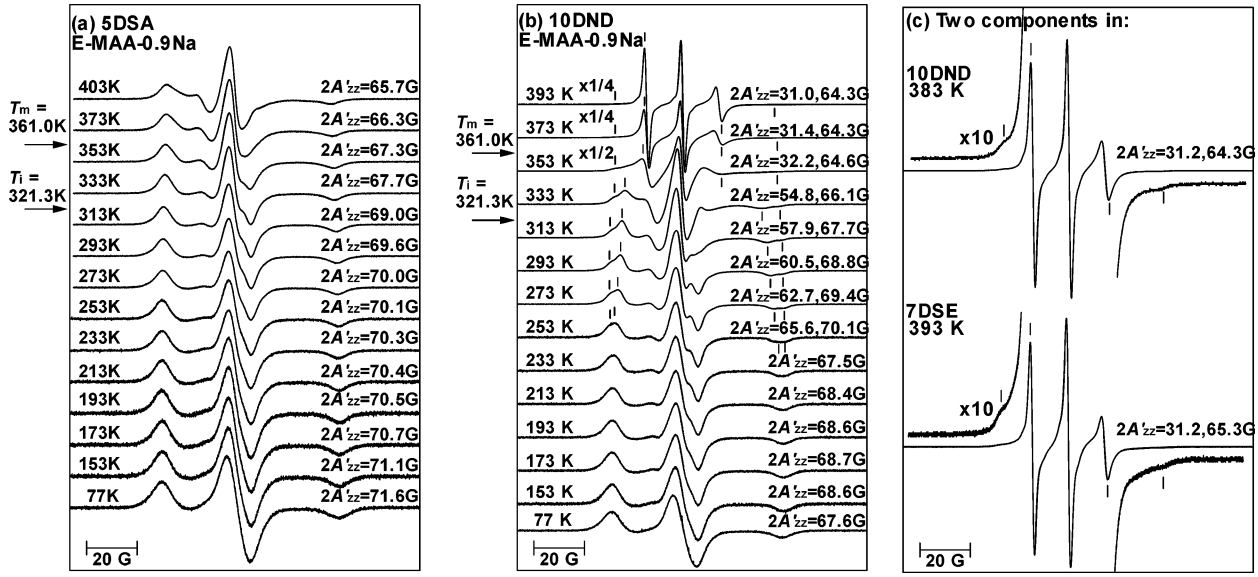

Figure 8. X-band ESR spectra of three probes in E−MAA-0.9Na: (a) 5DSA and (b) 10DND, as a function of temperature in the range of 77−403/393 K, and (c) two components of 10DND at 383 K (upper spectrum) and 7DSE at 393 K (lower spectrum). Two pairs of vertical bars in (b) and (c) at and above 253 K indicate two extreme separations corresponding to two spectral components (see text). The modulation amplitude was 0.1 mT.

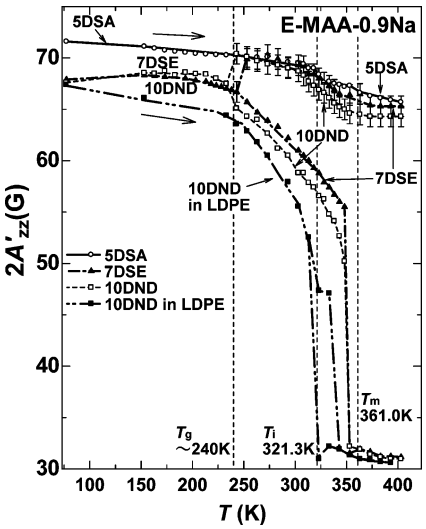

Figure 9. Plots of $2A'_{zz}$ vs T in the range 77−403 K on heating for 5DSA (○), 7DSE (▲), and 10DND (□) in E−MAA-0.9Na. T_g is the temperature at which the plots of $2A'_{zz}$ vs T for both 7DSE and 10DND begin to split, and T_i and T_m were determined by DSC. The data for 10DND in LDPE (■) are also shown for comparison.

The $2A'_{zz}$ values are almost equal to the value of 5DSA at the same temperature below ≈300 K, slightly below T_i, and above this temperature the magnitude of the decrease with temperature increases and then around T_m becomes gentle again. At 403 K, the $2A'_{zz}$ value of 10DND is 64.3 G and that of 7DSE is 65.3 G; the three values including that of 5DSA (65.7 G) indicate that the local molecular motions around these three probes are still strongly restricted at this temperature.

Our previous dielectric studies[34a] on E−MAA-xNa ionomers have provided the following insights into the molecular motions in the temperature range 77−400 K. For 0.2 ≥ x, two relaxations were observed at ≈190 and ≈320 K at a frequency of 1 kHz, both from the amorphous region. The low-temperature relaxation was assigned to a local molecular motion of short segments (labeled γ). The high-temperature relaxation was assigned to a micro-Brownian motion of long chain segments (labeled β'), which is thermally activated above the glass transition temperature T_g of the ionomer chains; the ionomer has one T_g. For $x \geq 0.4$, the β' relaxation is replaced with two relaxations, β at 282−294 K and α at 333−360 K, with their temperatures dependent on x. This replacement has generally been considered an indication of a microphase separation of ion-rich domains with its own T_g from the amorphous region, and the β relaxation is associated with the T_g of the matrix phase consisting of remaining polyethylene chains; the ionomer has two T_gs. The ion-rich domain was defined by Eisenberg and co-workers as the ionic cluster phase; in their model, the ionic cluster is a region containing a considerable amount of ionomer chains whose motions are strongly restricted by the aggregates therein (multiplets in their terminology).[26,37]

Splitting of two outer peaks seen for 7DSE and 10DND in E−MAA-0.9Na means the presence of two mobility states in the amorphous region, consistent with the dielectric observation mentioned above, and the immobile and mobile components of those probes are considered to come from the ionic cluster and matrix phases, respectively.

Discussion

What Changed at the Ionic Aggregate Transition at T_i? Our preceding paper[33] concluded that the spin probes used in this paper are reporters at different sites in E−MAA ionomers, depending on their polarity and the position of the radical site. The present studies have confirmed this conclusion by examining the $2A'_{zz}-T$ behavior of those probes; the results showed that the probes behave actually as "spin labels" at different sites in the ionomers when temperature is varied.

The $2A'_{zz}$ value of 5DSA monitors site dynamics inside the aggregate core on heating through T_i, which was found to be dependent on the neutralization level x of E−MAA-xNa: The plot for $x = 0.2$ showed no significant change around T_i, with no difference between the first heating scan after aging at room temperature for 30 days and the subsequent cooling and the second heating

scans (Figure 7). The plot for $x = 0.6$, on the other hand, exhibited a steplike decrease of ≈1.2 G at around T_i only on the first heating (Figure 5), and a similar steplike decrease of ≈1.4 G was seen for $x = 0.9$ (Figures 9 and 10). The change at T_i for both $x = 0.6$ and 0.9 indicates an increase in local molecular mobility inside the aggregate core and gives us a picture that above T_i the ability of the ionic aggregates to constrain the backbone chains attached to them weakens, and the ionic groups are inversely subjected to the thermal agitation from the backbones. Since the ionic aggregates themselves still exist above T_i, it may be said that the organization of the ionic aggregate partly melts and is transformed into a "disordered" state. This picture is consistent with our model of the ionic aggregate transition of E−MAA ionomers.[11−16,18,21] For $x = 0.2$ and $x = 0$ (the latter chart not included in the paper), unlike the cases for $x = 0.6$ and 0.9, the ability of the aggregate to constrain the mobility of surrounding chains is considered relatively low, and the influence that is given on the aggregate from the surroundings is also small. Hence, it is reasonable that the $2A'_{zz}$ vs T plot of 5DSA for $x = 0.2$ (and $x = 0$) shows no anomaly around T_i.

The DSC T_i peak takes place in the same manner for x in the range 0−0.9 except the size of the transition enthalpy. Considering this fact and the present ESR results, it seems likely that the transition at T_i undergoes somewhat in different ways between the ionomers of $0.2 \geq x$ and of $x \geq 0.4$; in the former ionomers, the contribution of the melting of imperfect polyethylene crystallites produced by room temperature aging to the T_i transition cannot be ruled out; the ionic groups would not be incorporated in the imperfect crystallites. With the same analogy, in the latter ionomers, the fact that in E−MAA-0.6Na (Figure 5) the $2A'_{zz}$ vs T plot of 10DND bends at around T_i seems to support the melting of imperfect crystallites model. In this case, however, the change at around T_i is more evident at the site of 5DSA, inside the ionic aggregate core. Moreover, the temperature behavior of 10DND is never in contradiction with the ionic aggregate transition model, considering that the ionic groups are connected with the ionomer backbones and both would be influenced by each other. Our previous dc conductivity studies excluded the possibility that the primary contribution to the T_i transition comes from the melting of imperfect crystallites not connected to ionic groups.[38] On the other hand, we also confirmed that the fully water-swollen aggregates still exhibit the T_i transition, although the transition enthalpy was largely (ca. 70%) reduced compared to the dry ionomer as expected from the ionic aggregate transition model.[15,28] From the latter fact, it is not realistic to consider that the T_i transition occurs solely in the ionic aggregate core regions. The present ESR results revealed a microscopic view that the T_i transition brings about changes in both ionic aggregate core and surrounding polyethylene regions. Probably, it is more realistic to consider that, in the latter ionomers, the T_i transition is a cooperative phenomenon associated with both ionic aggregates and some polyethylene organizations;[15,16] it should not be assigned to one contribution.

Difference in the Effect of Ionic Aggregation on the Chain Mobility between E−MAA-0.2Na, -0.6Na, and -0.9Na Ionomers. In comparison of Figures 4, 7, and 9, it is apparent that the difference between the $2A'_{zz}-T$ curves of five position-selective probes in the same ionomer becomes larger with increasing x. Such

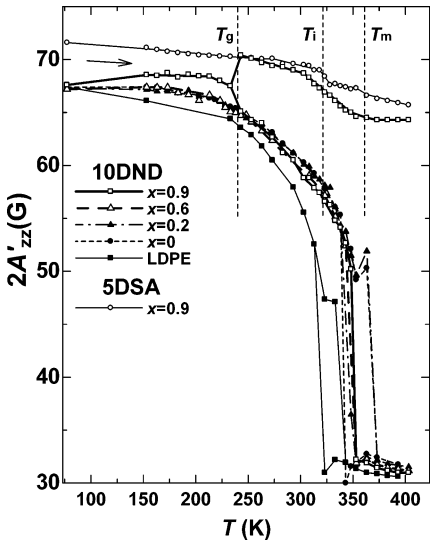

Figure 10. Plots of $2A'_{zz}$ vs T in the range 77−403 K on first heating for 10DND in LDPE (■), E−MAA-xNa ionomers with $x = 0$ (●), 0.2 (▲), 0.6 (△), and 0.9 (□), together with the behavior of 5DSA in E−MAA-0.9Na (○). T_g, T_i, and T_m have the same meaning as in Figure 9.

change with x reflects variation with x of the effect of ionic aggregation on the chain mobility in the system: For $x = 0.2$, the effect of ionic aggregates is only limited onto the chain segments incorporated in the aggregate cores, just around the probe site of 5DSA, whereas for $x = 0.6$, the region governed by the aggregates extends out over the regions where 7DSA and 10DSA reside. In both ionomers, however, immobilization of ionomer chains by the aggregates does not persist above T_m, the melting temperature of polyethylene lamellae. At much higher neutralizations such as $x = 0.8$ and 0.9, the ionic aggregates become to restrict the motions of ionomer chains in some areas of the amorphous region where hydrophobic 7DSE and 10DND are located. In fact, those spectra for $x = 0.8$ and 0.9 show the presence of two components with different $2A'_{zz}$ values, corresponding to two dynamical states in the amorphous region.

Figure 10 summarizes the $2A'_{zz}-T$ behavior of 10DND intercalated into the amorphous region of five polymers, LDPE, and E−MAA-xNa with $x = 0$, 0.2, 0.6, and 0.9, together with the behavior of 5DSA (within the ionic aggregate) in E−MAA-0.9Na for comparison. As mentioned, in phase-separated E−MAA-0.9Na ionomer, the local molecular motion in the cluster phase (where the immobile counterpart of 10DND is present) is restricted to the extent of the motion within the ionic aggregates. The mobility in the matrix phase, on the other hand, tends to be close to that in LDPE as x increases.

The promotion of the chain immobilization with increasing x has primarily been examined so far by macroscopic studies such as dynamic mechanical[34b] and dielectric studies,[34a] but as demonstrated in this paper, spin probe ESR is able to provide more microscopic and direct information on this subject.

Rearrangement Process during Room Temperature Aging and Stiffness Enhancement. It is well-known that the room temperature aging of E−MAA ionomers enhances the mechanical properties such as bending stiffness and surface hardness.[13,14,18] For example, under ≈0% relative humidity, the stiffness of E−MAA-0.6Na ($x = 0.6$) is 308 MPa at 3 day aging after cooling from the melt, which increases up to 386 MPa at 22 day aging.[18] The present studies have provided a

microscopic origin for this behavior. Figure 5 demonstrated that the room temperature aging caused further immobilization of chain segments almost everywhere in the sample, but especially within and in the vicinity of the ionic aggregate, resulting in the stiffness enhancement. It should be noted that the SAXS studies in Figure 6 were not able to detect any changes with aging time. In E−MAA-0.9Na, a similar microhardening was observed with aging time, but in this case, more prominent at the sites of the mobile counterparts of 7DSE and 10DND (in the matrix phase) (the chart not included in this paper). Such investigation would also be useful for understanding the microstructural change with aging time for other polymer systems.

Conclusions

The spin probe ESR method was applied to the study of dry membranes of E−MAA-*x*Na ionomers in the temperature range 77−403 K. Since the probes used for the study are known to be intercalated position selectively into the ionomers,[33] the temperature variation measurements are able to provide the dynamics information at each probe site.

The results have shown how the phase-separated structure is changed when temperature is varied on heating through three characteristic transition temperatures T_g, T_i, and T_m of the ionomers, which was dependent on the degree of neutralization x. The ESR probe site of 5DSA is located inside the aggregate core, and the $2A'_{zz}-T$ behavior for $x = 0.6$ and 0.9 elucidated the microscopic changes at the DSC T_i with a characteristic thermal hysteresis, in support of the model proposed by us.[11−16,18,21]

The difference of the $2A'_{zz}-T$ behaviors of five probes in the same ionomer was found to become larger with increasing x. This is interpreted as follows: The effect of ionic aggregates is only limited onto the aggregate core at $x = 0.2$, but at much higher neutralizations ($x =$ 0.8 and 0.9), the ionic aggregates become to restrict partially the chain mobility in the amorphous region, where hydrophobic 7DSE and 10DND are located, forming an ionic cluster phase. It was found that the chain immobilization in the cluster phase is reduced slightly around T_i but persists above T_m.

The spin probe ESR technique is useful and can be applied to other ionomer systems for studying their phase-separated structures.

Acknowledgment. We are first grateful to Prof. Shulamith Schlick of The University of Detroit Mercy (UDM), U.S.A., for valuable discussions and her comments; the use of amphiphilic spin probes was her idea. We are also grateful to Mr. Yoshikazu Kutsuwa and Mr. Tatsuya Watanabe of Du Pont-Mitsui Polychemicals Co., Chiba, Japan, for the gift of E−MAA ionomer samples; Dr. Eisaku Hirasawa of Fujimori-Kogyo Co., for helpful discussions and encouragement; and Prof. Takashi Kawamura of Gifu University, Japan, for his permission of our use of an ESR spectrometer; beamtime at PF−KEK was provided by Program 94G125. We appreciate the reviewers' constructive criticism for our manuscript. This work was partly supported by the Grant-in-Aid for Scientific Research on Priority Areas (A), "Dynamic Control of Strongly Correlated Soft Materials" (No. 413/13031037 and 14045232) from the Ministry of Education, Science, Sports, Culture and Technology, Japan.

References and Notes

(1) *Ionomers: Characterization, Theory, and Applications*; Schlick, S., Ed.; CRC Press: Boca Raton, FL, 1996.
(2) *Ionomers: Synthesis, Structure, Properties and Applications*; Tant, M. R., Mauritz, K. A., Wilkes, G. L., Eds.; Blackie Academic and Professional: London, 1997.
(3) Rees, R. W.; Vaughan, D. J. *Polym. Prepr. (Am. Chem. Soc., Div. Polym. Chem.)* **1965**, *6*, 287.
(4) Longworth, R.; Vaughan, D. J. *Nature (London)* **1968**, *218*, 85.
(5) Register, R. A.; Cooper, S. L. *Macromolecules* **1990**, *23*, 318.
(6) McLean, R. S.; Doyle, M.; Sauer, B. B. *Macromolecules* **2000**, *33*, 6541.
(7) Quiram, D. J.; Register, R. A.; Ryan, A. J. *Macromolecules* **1998**, *31*, 1432.
(8) Marx, C. L.; Cooper, S. L. *Makromol. Chem.* **1973**, *168*, 339.
(9) Marx, C. L.; Cooper, S. L. *J. Macromol. Sci., Phys.* **1974**, *B9*, 19.
(10) Tsujita, Y.; Shibayama, K.; Takizawa, A.; Kinoshita, T.; Uematsu, I. *J. Appl. Polym. Sci.* **1987**, *33*, 1307.
(11) Tadano, K.; Hirasawa, E.; Yamamoto, Y.; Yamamoto, H.; Yano, S. *Jpn. J. Appl. Phys.* **1987**, *26*, L1440.
(12) Tadano, K.; Hirasawa, E.; Yamamoto, H.; Yano, S.*Macromolecules* **1989**, *22*, 226.
(13) Hirasawa, E.; Yamamoto, Y.; Tadano, K.; Yano, S. *Macromolecules* **1989**, *22*, 2776.
(14) Hirasawa, E.; Yamamoto, Y.; Tadano, K.; Yano, S. *J. Appl. Polym. Sci.* **1991**, *42*, 351.
(15) Kutsumizu, S.; Nagao, N.; Tadano, K.; Tachino, H.; Hirasawa, E.; Yano, S. *Macromolecules* **1992**, *25*, 6829.
(16) Yano, S.; Tadano, K.; Nagao, N.; Kutsumizu, S.; Tachino, H.; Hirasawa, E. *Macromolecules* **1992**, *25*, 7168.
(17) Goddard, R. J.; Grady, B. P.; Cooper, S. L. *Macromolecules* **1994**, *27*, 1710.
(18) Tachino, H.; Hara, H.; Hirasawa, E.; Kutsumizu, S.; Yano, S. *J. Appl. Polym. Sci.* **1995**, *55*, 131.
(19) Ray, A. K. *J. Therm. Anal.* **1996**, *46*, 1527.
(20) Loo, Y.-L.; Register, R. A.; Hsiao, B. S. *Polym. Mater. Sci. Eng.* **1999**, *81*, 294.
(21) Kutsumizu, S.; Tadano, K.; Matsuda, Y.; Goto, M.; Tachino, H.; Hara, H.; Hirasawa, E.; Tagawa, H.; Muroga, Y.; Yano, S. *Macromolecules* **2000**, *33*, 9044.
(22) Kajiyama, T.; Stein, R. S.; MacKnight, W. J. *J. Appl. Phys.* **1970**, *41*, 4361.
(23) Kajiyama, T.; Oda, T.; Stein, R. S.; MacKnight, W. J. *Macromolecules* **1971**, *4*, 198.
(24) Uemura, Y.; Stein, R. S.; MacKnight, W. J. *Macromolecules* **1971**, *4*, 490.
(25) Szajdzinska-Pietek, E.; Schlick, S. In ref 1, Chapter 7, pp 135−163, and references therein.
(26) Tsagaropoulos, G.; Kim, J.-S.; Eisenberg, A. *Macromolecules* **1996**, *29*, 2222.
(27) Kutsumizu, S.; Hara, H.; Schlick, S. *Macromolecules* **1997**, *30*, 2320.
(28) Kutsumizu, S.; Schlick, S. *Macromolecules* **1997**, *30*, 2329.
(29) Schädler, V.; Franck, A.; Wiesner, U.; Spiess, H. W. *Macromolecules* **1997**, *30*, 3832.
(30) Szajdzinska-Pietek, E.; Pillars, T. S.; Schlick, S.; Plonka, A. *Macromolecules* **1998**, *31*, 4586.
(31) Pannier, M.; Schädler, V.; Schöps, M.; Wiesner, U.; Jeschke, G.; Spiess, H. W. *Macromolecules* **2000**, *33*, 7812.
(32) Pannier, M.; Schöps, M.; Schädler, V.; Wiesner, U.; Jeschke, G.; Spiess, H. W. *Macromolecules* **2001**, *34*, 5555.
(33) Kutsumizu, S.; Goto, M.; Yano, S.; Schlick, S. *Macromolecules* **2002**, *35*, 6298.
(34) For example: (a) Yano, S.; Nagao, N.; Hattori, M.; Hirasawa, E.; Tadano, K. *Macromolecules* **1992**, *25*, 368. (b) Tachino, H.; Hara, H.; Hirasawa, E.; Kutsumizu, S.; Tadano, K.; Yano, S. *Macromolecules* **1993**, *26*, 752.
(35) Kutsumizu, S.; Tagawa, H.; Muroga, Y.; Yano, S. *Macromolecules* **2000**, *33*, 3818 and references therein.
(36) *Physical Properties of Polymers Handbook*; Mark, J. E., Ed.; AIP Press: Woodbury, NY, 1996.
(37) Eisenberg, A.; Hird, B.; Moore, R. B. *Macromolecules* **1990**, *23*, 4098.
(38) Kutsumizu, S.; Hashimoto, Y.; Hara, H.; Tachino, H.; Hirasawa, E.; Yano, S. *Macromolecules* **1994**, *27*, 1781.

MA0305885